



Proceedings of the  
Estonian Academy of Sciences  
2025, 74, 2S, 281–290

<https://doi.org/10.3176/proc.2025.2S.02>

[www.eap.ee/proceedings](http://www.eap.ee/proceedings)  
Estonian Academy Publishers

## POWER ELECTRONICS

### RESEARCH ARTICLE

Received 19 December 2024  
Accepted 2 April 2025  
Available online 21 May 2025

#### Keywords:

Power electronics, DC microgrid,  
solid-state circuit breaker, overcurrent  
protection, residual current detection

#### Corresponding author:

Tanel Jalakas  
[tanel.jalakas@taltech.ee](mailto:tanel.jalakas@taltech.ee)

#### Citation:

Jalakas, T., Chub, A., Roasto, I.,  
Vinnikov, D. and Kurnitski, J. 2025. Design  
and development of solid state circuit  
breaker with residual current protection for  
residential prosumer DC microgrids.  
*Proceedings of the Estonian Academy of  
Sciences*, 74(2S), 281–290.  
<https://doi.org/10.3176/proc.2025.2S.02>

© 2025 Authors. This is an open  
access article distributed under the  
terms and conditions of the Creative  
Commons Attribution (CC BY) license  
(<http://creativecommons.org/licenses/by/4.0>).

# Design and development of solid state circuit breaker with residual current protection for residential prosumer DC microgrids

Tanel Jalakas<sup>a</sup>, Andrii Chub<sup>a</sup>, Indrek Roasto<sup>a</sup>, Dmitri Vinnikov<sup>a</sup>  
and Jarek Kurnitski<sup>b</sup>

<sup>a</sup> Department of Electrical Power Engineering and Mechatronics, Tallinn University of  
Technology, Akadeemia tee 3, 19086 Tallinn, Estonia

<sup>b</sup> Department of Civil Engineering and Architecture, Tallinn University of Technology,  
Ehitajate tee 5, 19086 Tallinn, Estonia

## ABSTRACT

DC microgrids require rapid and reliable techniques for residual current detection and protection against short circuit, overcurrent, and overvoltage. Solid-state circuit breakers provide viable high-speed protection for DC microgrids. Microcontroller-based control circuits, in conjunction with a diverse array of sensors, facilitate rapid fault identification, measurement of various grid parameters, telemetry, and load control, while metal-oxide-semiconductor field-effect transistor based switching cells enable swift isolation of these faults. A device that integrates bidirectional solid-state circuit breaker (SSCB) and residual current device (RCD) features into a single hybrid unit is required to safeguard users and linked apparatus. Only a limited number of proven solutions for measuring residual current can be directly utilized in DC grids. Hall effect sensors offer low power consumption and compact physical dimensions. Nonetheless, fluxgate-based current sensors provide enhanced linearity and precision. Therefore, a hybrid SSCB/RCD protection device that operates as such is proposed in this paper. The primary design and implementation challenges of DC microgrids and various residual current measurement techniques were examined to assess the proposed hybrid device. The power circuit topology was selected, and a compact prototype was developed and evaluated in the laboratory. Conducted tests demonstrated its conformance with requirements, usefulness in residential 350 V DC microgrids, and capability to safeguard the microgrid from short circuits, users from electric shock, and the grid from overloads caused by connected devices.

## 1. Introduction

In line with the tendency to enhance energy efficiency across all sectors of the economy, the demand for residential energy efficiency has notably increased [1]. A future shift to zero-emission buildings necessitates extensive electrification. New technologies for local renewable energy generation, storage, and energy management are required to achieve this. One of the most promising strategies is the replacement of alternating current (AC) power distribution systems with direct current (DC) alternatives [2–4]. Buildings with DC power distribution systems can enable optimal use of on-site energy generation and substantially enhance overall energy efficiency. Introducing new technologies, such as DC power distribution, raises issues related to the safety of users and connected devices, and necessitates further research into dedicated protection devices. Dedicated DC-rated control and protection devices, such as circuit breakers, residual current devices, overvoltage detectors, dataloggers, telemetry, and load control modules, are required for emerging DC microgrids in small commercial buildings and smart districts [5–8]. Available protection systems designed for AC operation are not directly suitable for use in DC microgrids; thus, specialized DC-ready devices are needed.

Recent developments in semiconductor and packaging technologies allow for the integration of all these control and protection functions into a single compact, DC-rated bidirectional circuit breaker. Modern microcontrollers, miniaturized sensors, and telecommunication modules enable seamless measurement, logging, and telem-

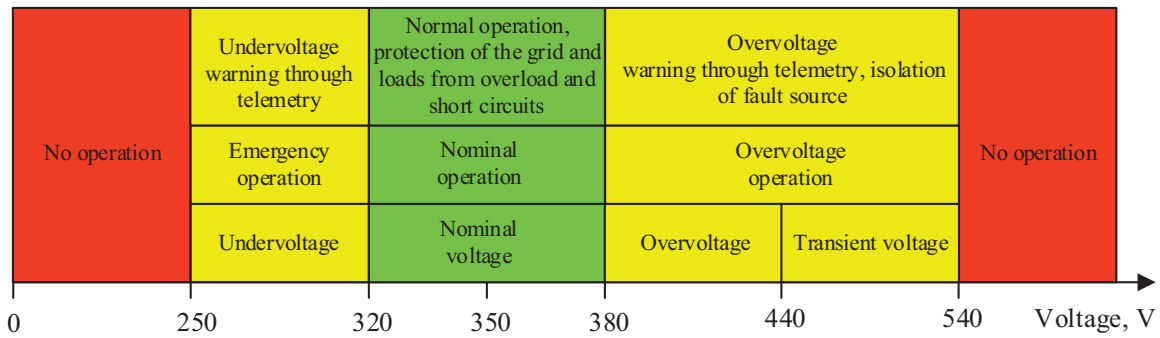


Fig. 1. Voltage bands for residential DC microgrid.

etry of grid voltage, load current, device status, and more. Fast, bidirectional semiconductor-based switching cells offer significantly faster fault isolation and more flexible load control than melting fuses and electromechanical circuit breakers. Arc-less fault current disconnection by the solid-state circuit breaker increases both the reliability and longevity of the protection system, thus improving the overall electrical safety of DC microgrids.

The main design and implementation challenges of solid-state circuit breakers (SSCBs) in residential DC buildings nowadays include adaptation to a specific voltage range, selection of proper current ratings, and compliance with short-circuit interruption speed and current level requirements. Additional challenges involve integration versatility by introducing functions such as data communication, telemetry, and remote load control. Another key design issue for such integrated devices is the implementation of residual current measurement technology that is compatible with direct current. Technologies such as fluxgate, Hall effect, or giant magnetoresistance (GMR) sensors must be considered, as typical AC-based current sensor technologies, such as current transformers and Rogowsky coils, are not applicable.

The existing protection devices for DC microgrids have been evaluated and compared in [9–14], revealing a lack of solutions specifically designed for residential DC microgrids. Therefore, a preliminary study of a residential DC SSCB with embedded residual current device (RCD) functionality was first discussed in [15], which serves as the basis for the further development presented in this paper. This paper introduces a bidirectional SSCB/RCD hybrid intended for application in residential prosumer DC microgrids, along with additional analysis of circuit breaker implementation challenges and a more comprehensive experimental study. The paper is structured into four principal sections. The first section details the design specifications for the DC grid side of the SSCB, including grid voltage range, current ratings, and short-circuit interruption criteria. The second section addresses feasible residual current measurement methods in DC microgrids. The third section presents a technical solution for a DC-rated solid-state circuit breaker prototype that incorporates integrated control and protection capabilities. The final section presents an investigation of the experimental prototype, accompanied by a brief explanation of the test results.

## 2. Circuit breaker implementation issues for residential prosumer DC microgrids

### 2.1. Voltage range

Residential DC buildings involve the integration of multiple energy sources, loads, and energy storage systems. The appliances and electrical equipment in DC buildings are expected to operate at a standardized nominal voltage level of 350 VDC [16,17]. The minimum and maximum grid voltage levels are fixed at 320 and 380 V, respectively [18,19]. The voltage range between 320 and 250 V is defined as the emergency low-voltage band, while the range from 380 to 540 V is classified as the overvoltage band. Within the overvoltage band, 380 to 440 V is designated for allowed overvoltage events, and 440 to 540 V is defined for short-term voltage transients, as shown in Fig. 1.

It can be concluded that circuit breakers used in residential DC buildings with a 350 V bus must be able to operate within a range of 250 to 440 V and withstand transient voltages up to 540 V. Moreover, prosumer buildings require bidirectional current flow and breaking capabilities. Switching elements must have bipolar voltage-blocking capabilities with a rated voltage of >540 V due to inductive overvoltage pulses that occur after short-circuit interruption. For example, the metal-oxide-semiconductor field-effect transistors (MOSFETs) employed in SSCBs for residential DC buildings should have a drain-source breakdown voltage rating of at least 600 V. Moreover, bidirectional current-blocking capability requires a back-to-back connection of two MOSFETs. This implementation drawback could be resolved with the emergence of monolithically integrated bidirectional switches, which have recently entered the market but still have limited availability and a variety of parameters. The auxiliary power supply of such a protection device must be operational from 250 to 440 V, and it must be protected from 540 V transients using properly selected varistors, bypass capacitors, and similar components. Undervoltage conditions must be reported through the SSCB's telemetry channel; when an overvoltage condition appears, the fault source must be isolated, and a telemetry report must be generated.

### 2.2. Current ratings

The connected loads and the maximum allowable current of the wiring usually define the circuit breaker's current rating.

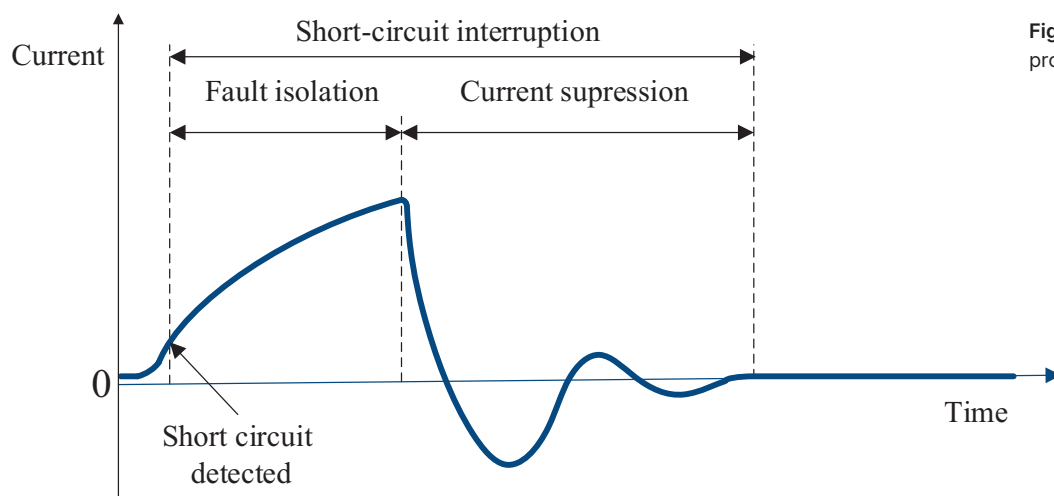


Fig. 2. Short-circuit interruption process.

Copper power cables installed inside the wooden walls of a residential house, between thermal insulation layers, can be rated for different typical currents. For example, copper wires with a cross-section of  $1.5 \text{ mm}^2$  have a maximum allowed current-carrying capacity of 13 A and are typically used with breakers rated for 10 A, while  $2.5 \text{ mm}^2$  wires are used with 16 A-rated breakers, etc. [20]. Wires of  $1.5 \text{ mm}^2$  are typically used to supply lighting systems, while more powerful loads, such as power sockets, heaters, ovens, washing machines, and heat pumps, are wired with  $2.5 \text{ mm}^2$  wires connected to 16 A circuit breakers. At 16 A, a 350 V DC grid can deliver 5.6 kW of power, which is more than enough for most residential appliances and other equipment, while 32 A can deliver up to 11.2 kW, which is sufficient for most residential households if larger appliances are used in a well-synchronized manner [21]. To cover even higher power, a 700 V uni- or bipolar DC grid can be used [16], where a 32 A breaker enables up to 22.4 kW of electrical power to be delivered. This means that the current ratings of circuit breakers used in residential DC buildings could range from 1 to 32 A, covering most residential needs.

Another important feature of bidirectional SSCBs for residential DC buildings is the short-circuit current rating (SCCR). SCCR defines the maximum current value that the protection device must withstand until it opens and clears the fault. The short-circuit maximum value is determined by the grid voltage, capacitance, inductance, wire resistance, and the short-circuit interruption time of the protection device [22,23]. SSCBs can react to a short-circuit in less than  $10 \mu\text{s}$  [24], which allows to limit the short-circuit current in a DC grid to below several hundred amperes. In contrast, slower electromechanical protection devices must have an SCCR of several kiloamps [25] to withstand short circuits without damaging the installation or connected devices. For example, the SCCR of the Schneider Electric A9N61531 C60H-DC C16A breaker is 6 kA at 500 VDC [26]. The short-term current pulse ratings of electromechanical relays are usually much lower, limiting the use of electromechanical relay-based circuit breakers in critical parts of a DC grid. Often, the short-circuit current amplitude is limited by the amount of energy stored in the total capacitance of a DC microgrid.

As SSCBs are envisioned to be housed in switchboards, similar to AC breakers, energy dissipation is an important

consideration for switchboard thermal management. Therefore, MOSFETs used in SSCBs must have low on-state resistance to reduce losses in the device during normal operation and to enable a high maximum current pulse value needed to avoid catastrophic damage during short-circuit fault interruption. This becomes even more challenging for bidirectional SSCBs designed for prosumer DC buildings, as they typically use two power semiconductor devices in the current path, doubling the conduction losses.

### 2.3. Short-circuit interruption

The short-circuit current and the potential damage to devices and the grid are reduced when the short-circuit interruption time is reduced. Theoretical limits on the SSCB short-circuit interruption time are set by the properties of the switching elements, drivers, measurement, and control circuits. The interruption time consists of several intervals: the fault isolation time, which is dependent on the protection device, and the current suppression time, which depends on the properties of the microgrid (Fig. 2). Further analysis of short-circuit faults and the protection of DC microgrids is covered in [28,29].

Gallium nitride (GaN) and silicon carbide (SiC) transistors enable very short fault interrupt times [24], but delays in current measurement and control logic limit the reaction time of SSCBs in most implementations to 1 to  $10 \mu\text{s}$  [30,31]. From a practical point of view, SiC devices are more suitable for these applications as they have well-defined avalanche ratings, while high-electron-mobility GaN devices are typically not avalanche-rated. In contrast, the short-circuit interruption time (electromagnetic tripping) of electromechanical circuit breakers (EMCBs) can range from 1 ms to 5 s in extreme cases, depending on the required tripping characteristic [11]. This delay arises from the much slower electromagnetic overcurrent tripping mechanism and mechanical contacts, so the fault isolation time also includes contact opening time and arcing duration. The short-circuit current rating and interruption time of SSCBs and EMCBs are visualized in Fig. 3.

### 2.4. Telemetry

New circuit breakers for residential DC buildings with an active microcontroller-based control system should also include telemetry capabilities. Telemetry enables the monitoring of important parameters of the grid and connected devices

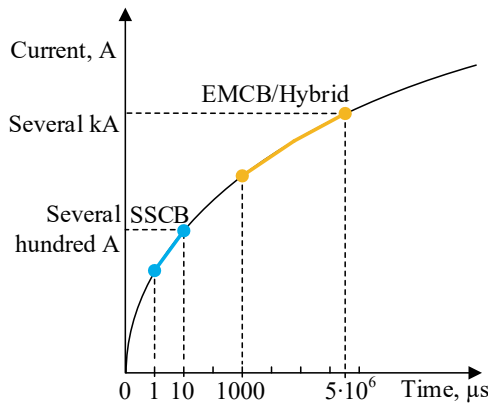


Fig. 3. SSCB and EMCB short-circuit interruption time, current, and ratings for residential DC microgrids.

(voltage, current, power, consumed energy), generates warnings and fault logs, and facilitates higher-level load control (remotely switching loads on and off). There are several options for connecting the device to higher-level supervisory control and data acquisition (SCADA), control, and monitoring systems (Table 1) [32,33].

Universal asynchronous receiver-transmitter (UART) is a low-cost and simple solution that is typically integrated into most microcontrollers at the hardware level. However, it is slow and has poor electromagnetic noise tolerance, limiting its practical use. Despite being similar to UART, RS-485 has much better noise resilience due to differential implementation at the physical level, so its range can be extended to hundreds of meters while lowering the data transfer speed. The controller area network (CAN) bus has reasonable speed, but the number of devices connected to it is limited, along with an effective range of <40 m. On the other hand, MODBUS is a simple and scalable solution, making it widely used in automatic control systems where its relatively slow data transfer speed is acceptable. Wired and wireless Ethernet offers high data transfer speed, high flexibility, simple connection to the internet, and versatility, as Ethernet devices are widely used. Wireless LAN devices are even more flexible and comfortable to install, but the concerns are higher data delays and possible security issues. UART, RS485, and CAN bus could be used for communication between devices in local installations. MODBUS is preferred in industrial settings where simple connectivity to industrial controllers and SCADA devices is needed. Ethernet-based devices are good for residential use due to their high data transfer speed, versatility, connection simplicity, and abundance of existing

Ethernet infrastructure. Critical systems should be connected through wired connections due to cybersecurity and electromagnetic interference issues. Bluetooth is good for connecting devices locally with smart handheld devices but lacks range (<10 m). Conversely, LoRaWAN has a very good range (up to 15 km) but slow data communication speed and high latency, limiting its usefulness. At the software communication protocol level, MQTT, REST, WebSocket, or other alternatives could be used to ensure compatibility with other systems and software used for control, monitoring, data logging, and process visualization. Despite abundantly available protocols, one of the major obstacles is the lack of a well-defined standardized data exchange model, limiting the design of smart DC devices to custom communication implementations.

2.5. Power density

The power density of circuit breakers is an important parameter in residential DC buildings, as the volume of electrical installation cabinets is limited. The electrothermal circuit breaker has the highest power density, as it does not need a complicated control or cooling system. The thermal and magnetic trip mechanisms, electrical contacts, and anti-arc chamber are relatively compact. Electromechanical relay-based circuit breakers require additional control, measurement, and auxiliary supply systems, which decreases their power density. SSCBs need control, an auxiliary power supply, measurement, cooling, and snubber circuits to protect the switching elements, further decreasing the power density. However, advancements in semiconductor technology (wide band-gap MOSFETs with better properties) [34–36] and power electronics help minimize losses, miniaturize devices, and increase power density. The lowest power density is typically found in hybrid circuit breaker topologies that integrate electrothermal and solid-state circuit breaker technologies.

3. Residual current detection

Only a limited number of proven solutions for measuring residual current can be directly utilized in residential DC microgrids. Current measurement methods, such as current transformers and Rogowski coils, are used in AC grids but are inapplicable to DC grids. A fluxgate, Hall effect sensor, or alternative active sensor technology is necessary to measure the minute leakage currents in DC grids. These sensors are available in several types: open-loop and closed-loop Hall

Table 1. Physical telemetry channels for circuit breakers

Physical telemetry channel	Advantage	Disadvantage
Universal asynchronous receiver-transmitter	Simple hardware	Slow speed, low range
UART and RS-485	Noise resilience and simple hardware	Slow speed, good range
CAN	Reasonable speed	Limited count of devices
MODBUS	Simple and scalable	Slow speed
Wired Ethernet	High speed	High delay
Wireless LAN	High speed, flexibility	High delay, security issues
LoRaWAN	Range	Slow speed, high latency
Bluetooth	Flexibility	Low range

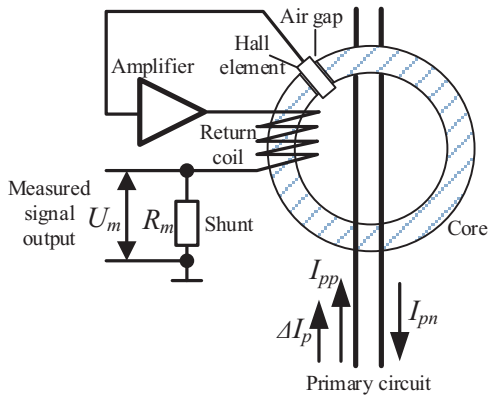


Fig. 4. Hall effect-based current sensor.

effect, open-loop fluxgate, and self-oscillating open- or closed-loop fluxgate sensors, etc.

The fundamental idea behind Hall effect sensors (Fig. 4) is that a voltage, referred to as the Hall voltage  $V_H$ , is generated across a Hall element when it is exposed to a magnetic field parallel to the direction of current flow.  $V_H$  is calculated with the following equation, where  $I_{pp}$  and  $I_{pn}$  are currents,  $B$  is the magnetic field intensity, and the constant  $R_H$  is the Hall coefficient [37]:

$$V_H = \frac{R_H}{d} (I_{pp} - I_{pn}) B, \quad (1)$$

where  $d$  represents the thickness of the semiconductor material in the Hall element. The primary benefits of Hall effect current sensors are minimal power consumption and compact size. The merits and demerits of Hall effect sensors are examined in [38–40].

Fluxgate-based current sensors have superior linearity and precision, making them the preferred option for DC-grid RCD implementation. A standard fluxgate sensor (Fig. 5) has a toroidal magnetic core and an excitation coil. In a self-oscillating fluxgate sensor, the magnetic core is produced without an air gap. The single-turn primary windings of the measured currents traverse the magnetic core. In contrast, the secondary winding comprises an excitation coil (with a turn count of  $N_s$ ) and a shunt resistor ( $R_s$ ). A square wave voltage signal  $U_s$  energizes the RL (resistor-inductor) circuit, de-

signed so that the inductor current ( $I_s$ ) escalates to the saturation point of the magnetic core – characterized by magnetic path length  $l_e$ , saturation flux density  $B_{sat}$ , and relative permeability ( $\mu_r$ ) – during each half cycle. The amplitude of the excitation current  $I_s$  will rapidly increase due to the reduction in inductance  $L_s$  of the excitation coils (with core cross-sectional area  $A_e$ ), resulting in brief alternating current pulses [12]:

$$L_s = \frac{\mu_0 \mu_r N_s^2 A_e}{l_e}, \quad (2)$$

$$I_s = \frac{l_e H_{sat}}{N_s} \approx \frac{l_e B_{sat}}{\mu_0 \mu_r N_s}. \quad (3)$$

The signal is altered when direct currents  $I_{pp}$  and  $I_{pn}$ , differing by  $\Delta I_p$ , traverse a primary winding, generating a magnetic field:

$$I_{pn} = I_{pp} + \Delta I_p. \quad (4)$$

To quantify the difference between the currents flowing through the conductors and measure their DC value, specialized signal processing algorithms are employed, as the second harmonics of the excitation coil current correlates with the current in the primary winding.

The analysis of second harmonics necessitates complex computations using a powerful microcontroller, which leads to substantial power consumption, hence increasing the cost of the circuit breaker and diminishing its overall efficiency.

The self-oscillating fluxgate sensor is an economical solution, where an astable multivibrator, comprising an RL circuit and an inverted Schmitt trigger, produces the oscillating square wave signal for the excitation coil. The average value of the excitation current waveform is directly proportional to the average value of the primary current. A simple RC circuit can be used to create a low-pass filter for direct measurement via a microcontroller's ADC input. The principal disadvantage of the self-oscillating sensor is the nonlinear relationship between the primary current and the average excitation current values. This problem can be addressed by employing a simple algorithm and lookup table within the circuit breaker control system and/or the feedback circuit in a closed-loop sensor configuration [41].

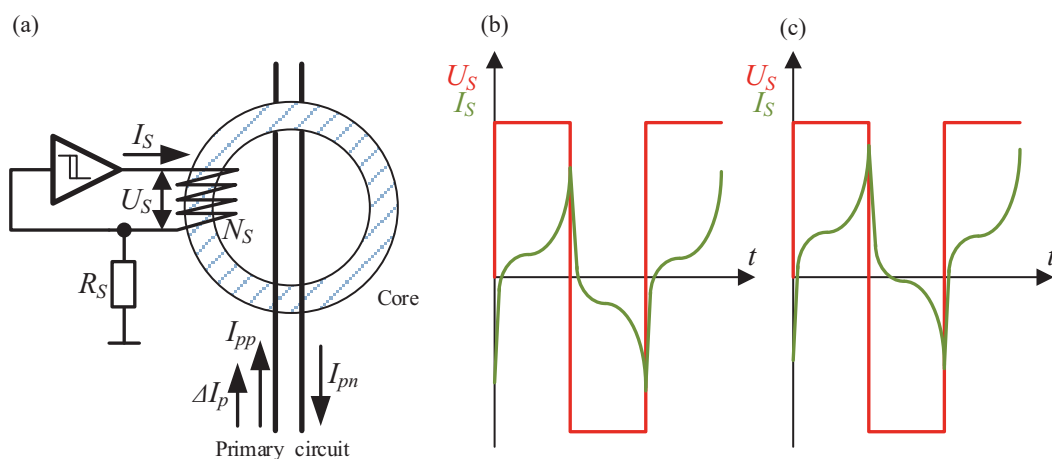


Fig. 5. Self-oscillating open-loop fluxgate sensor (a), excitation coil voltage and current (b), excitation coil current shift caused by  $\Delta I_p$  (c).

Basic fluxgate sensors exhibit significant disadvantages, including the periodic saturation of the measurement coils due to fluxgate excitation. To address this issue, the current sensor design must be altered to incorporate a secondary core with a reversed polarity winding. An additional RL circuit, which powers this winding, helps mitigate the noise generated by the detection of coil saturation when subjected to an excitation voltage.

Among the economical DC-capable residual current detection technologies, the GMR approach has significant zero current signal drift and comparatively low precision [42,43]. However, recent advancements in magnetic materials have facilitated the invention of more sophisticated detection systems, such as magnetic modulation [44].

Last but not least, the implementation of the RCD functionality must consider the bidirectional current flow in prosumer DC buildings.

#### 4. General technical concept

The proposed bidirectional SSCB/RCD hybrid comprises five fundamental parts: the control system, auxiliary power supply, current measurement, residual current monitoring, and the main solid-state current breaking element, which also includes a driver and snubber, as shown in Fig. 6a. The main current breaking component must have a low on-resistance ( $R_{DS(ON)}$ ) to minimize losses and facilitate rapid ( $<1 \mu s$ ) disconnection. A bidirectional semiconductor switching cell is necessary in SSCBs for grid-integrated battery energy storage systems, supercapacitor-based storage, and other devices capable of supplying energy to the grid.

Standard residential DC grid voltages of 350 and 700 V can be employed with suitable driver circuits and high-performance MOSFETs that exhibit adequate dynamic and static characteristics. R-C or R-C-D snubber circuits mitigate the impact of short-circuit interruptions, including high-voltage transients caused by the inherent inductance of the DC grid. For a typical 350 V DC grid, MOSFETs rated for at least 600 V, together with supplementary snubber circuits, are necessary to limit voltage stress during current breaking operations.

Shunt resistors are frequently utilized with high-speed signal amplifiers to achieve the needed rapid measurement speeds. Modern measurement and control systems must guarantee rapid current measurement and circuit disconnection times while minimizing losses. Fault detection can be accomplished either by using a slower microcontroller in combination with an external comparator and trigger circuit (Fig. 6b), or a faster microcontroller equipped with an internal comparator.

The approach for disconnecting the short-circuit source comprises three fundamental steps. In the initial stage, the fault current increases, limited by the grid inductance. The second step commences when the measured current exceeds a specified threshold, deactivating MOSFETs  $Q1$  and  $Q2$ . Diode  $D_{s1}$  is then utilized to charge capacitor  $C_{s1}$ . In the final stage, resistor  $R_{s1}$  dissipates the energy stored in  $C_{s1}$ . The amplitude of the short-circuit current  $i_p$  is calculated using the following equation [45,46]:

$$i_p = k \cdot K_c \cdot \frac{U_{grid}}{R_{total}}, \quad (5)$$

where  $k$  represents the approximation factor, and  $U_{grid}$  denotes the DC microgrid voltage across  $C_{total}$ . The variable  $K_c$  can be determined as:

$$K_c = \frac{2\delta}{|\omega_d|} \cdot \sinh(|\omega_d| \cdot t_p) e^{-\delta \cdot t_p}, \quad (6)$$

where

$$\delta = \frac{R_{total}}{2L_{total}}, \quad (7)$$

$$\omega_0 = \sqrt{\frac{1}{L_{total} \cdot C_{total}}}, \quad (8)$$

$$\omega_d = \sqrt{\delta^2 + \omega_0^2}. \quad (9)$$

The combined resistance, inductance, and capacitance of the DC microgrid are denoted as  $R_{total}$ ,  $L_{total}$ , and  $C_{total}$ , respectively. The duration of the short-circuit peak value,  $t_p$ , is calculated as follows:

$$t_p = \frac{1}{2|\omega_d|} \cdot \ln \left( \frac{\delta + |\omega_d|}{\delta - |\omega_d|} \right). \quad (10)$$

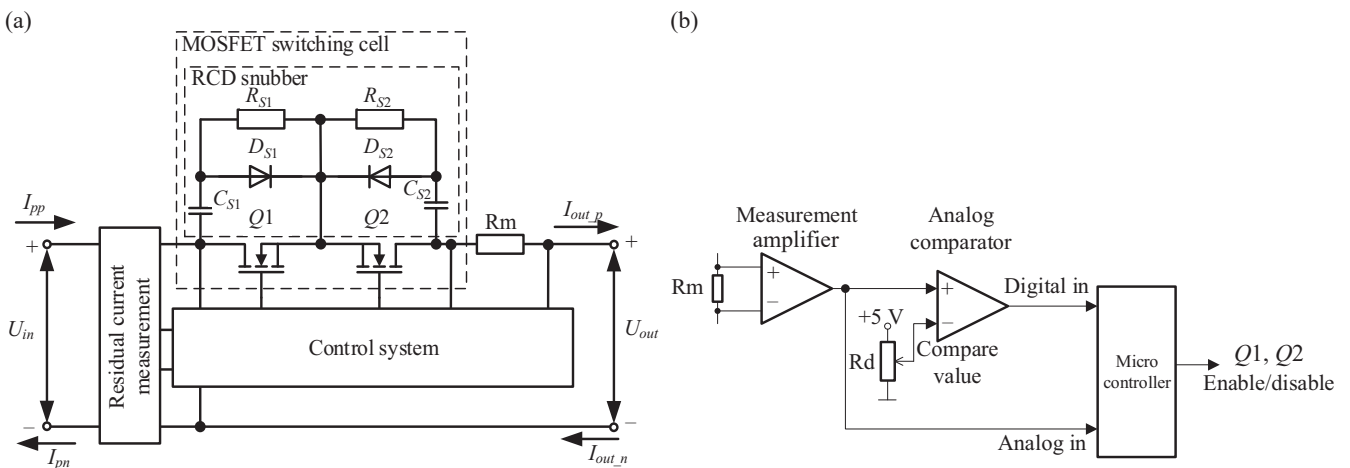


Fig. 6. Power circuit of the proposed bidirectional SSCB/RCD hybrid (a) and short-circuit detector of the SSCB (b).

## 5. Prototype and experimental results

The proposed bidirectional SSCB/RCD hybrid prototype, shown in Fig. 7a, comprises the components listed in Table 2. This prototype can mitigate direct short circuits, overload pulses, and light overloads of extended duration. When the current exceeds 48 A, short-circuit protection engages almost immediately ( $<10 \mu\text{s}$ ), whereas overload protection adheres to the standard B characteristics. This is necessary to allow brief current transients, such as those arising during motor start-up or the connection of powerful devices. The residual current protection algorithm permits leakage currents of up to 6 mA before disconnecting the fault source from the DC grid.

Employing MOSFETs with minimal on-state resistance reduces conduction losses in the SSCB. Short-circuit and overload currents are quantified using a current-sensing shunt resistor, while a closed-loop fluxgate sensor is employed to assess residual current. An external analog comparator circuit ensures a rapid response in the event of a direct short circuit.

A laboratory configuration emulating a 350 V residential DC microgrid was established to assess the experimental DC grid protection system. The setup includes a prototype circuit breaker, an external power supply, a capacitor, an electro-mechanical relay to trigger a short circuit, a load resistor, a 0.8 mF capacitor, and an external 9  $\mu\text{H}$  inductor to replicate the capacitance and line inductance of a DC microgrid, as illustrated in Fig. 7b. The elevated grid capacitance emulates the input or output capacitance of grid-connected apparatus, such as power supplies and DC loads.

In the initial test, two 87.5 k $\Omega$  resistors,  $R_{leak1}$  and  $R_{leak2}$ , were incorporated into the configuration to establish resi-

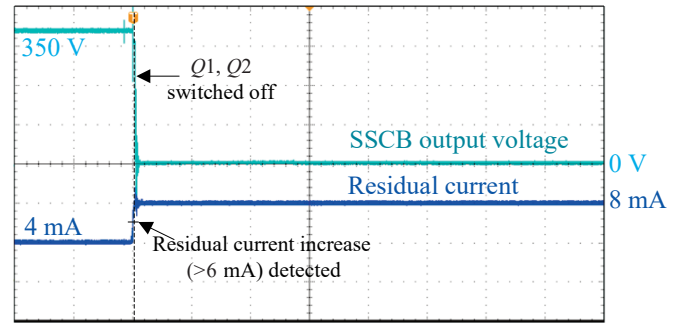


Fig. 8. SSCB residual overcurrent ( $>6 \text{ mA}$ ) test (timescale: 200  $\mu\text{s}/\text{div}$ ).

dential current levels of 4 and 8 mA. Initially, only the  $R_{leak1}$  was connected to the 350 V DC bus to replicate the normal leakage currents caused by interconnected devices, EMI filters, and similar components. Subsequently,  $R_{leak2}$  was incorporated in parallel with  $R_{leak1}$  to increase the residual current level and simulate a possibly hazardous electric shock to a DC grid user. As illustrated in Fig. 8, the SSCB isolates the fault source upon detecting an increase in residual current.

A further test confirms the short-circuit detection capability. First, the microprocessor activates the MOSFET drivers after SSCB initialization. An independent electro-mechanical relay is then employed to short-circuit the emulated DC microgrid after the SSCB has been activated.

Figure 10 presents the results of the short-circuit test. The trigger level for short-circuit protection is established at 48 A (three times the nominal current) by configuring the comparator's negative input voltage via a voltage divider.

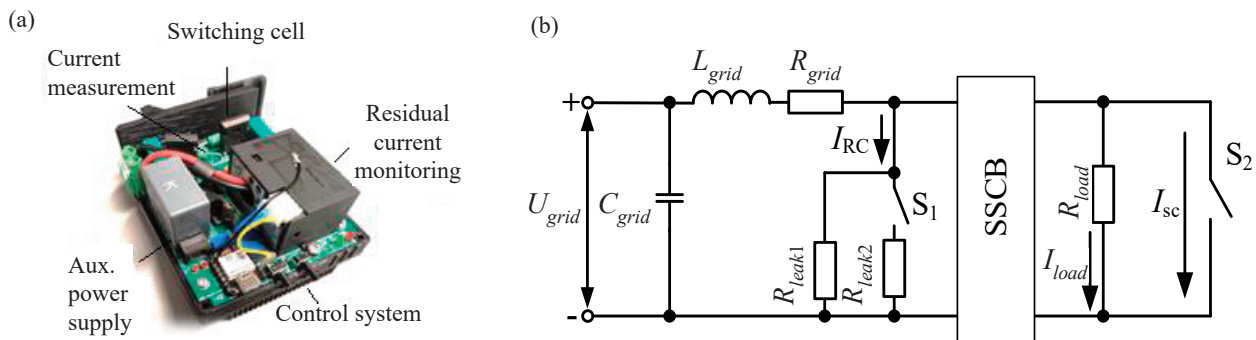


Fig. 7. Bidirectional SSCB/RCD hybrid prototype (a) and DC microgrid laboratory setup used for short-circuit and residual current detection evaluation (b).

Table 2. Specifications of the prototype

Parameter	Value
Nominal voltage	350 V
Nominal current	16 A
Max. short-circuit current	360 A
Residual current limit	6 mA
DC grid capacitance	0.8 mF
DC grid inductance	9 $\mu\text{H}$
$D_{S1}, D_{S2}$	Wolfspeed/Cree C4D30120H
$Q1, Q2$	Infineon IPW60R024CFD7XKSA1
Microcontroller	XIAO-ESP32C3
Load current measurement	0.001 $\Omega$ shunt with AD8210 operational amplifier
Residual current measurement	Western Automation RCM14-01, closed-loop, self-oscillating fluxgate current sensor

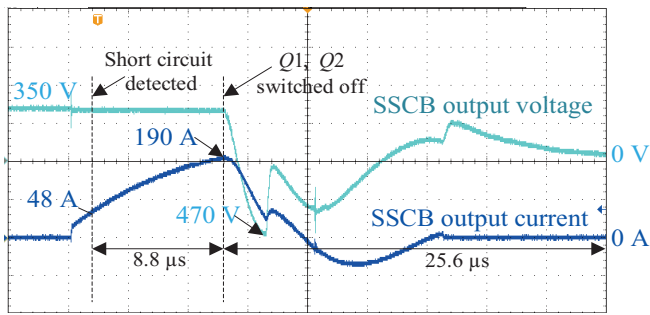


Fig. 9. SSCB short-circuit protection test (timescale: 4  $\mu$ s/div).

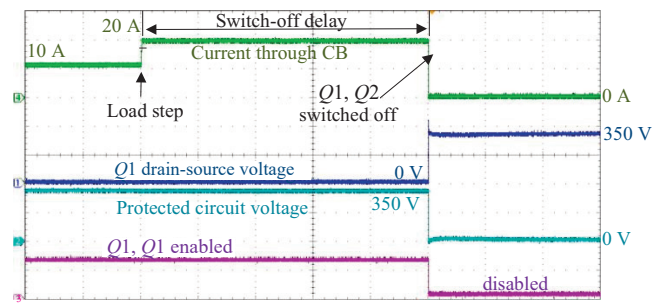


Fig. 10. SSCB overload protection test (timescale: 0.2 s/div).

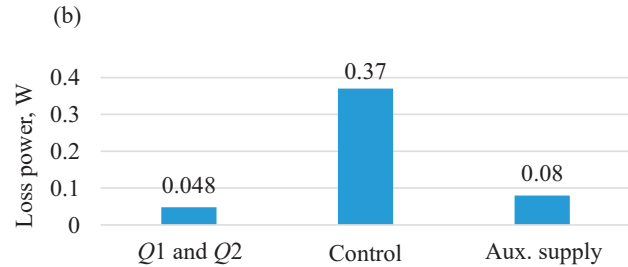
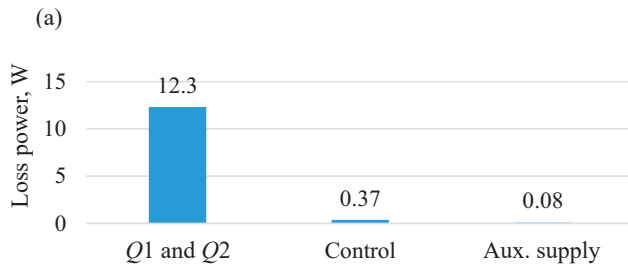


Fig. 11. SSCB power loss breakdown (a) at nominal load (16 A, 350 V) and (b) at light load (1 A, 350 V).

The microprocessor responsible for activating or deactivating the MOSFETs monitors the output of the comparator. The SSCB automatically disconnects when the current exceeds 48 A and the comparator output reaches 3.3 V. An experimental short-circuit amplitude of 190 A is recorded, caused by delays in the measuring circuit, microcontroller, and transistor driver (all  $<10 \mu$ s). The overvoltage pulse, characterized by an amplitude of 470 V and a duration of 2  $\mu$ s, is attributed to grid inductance. The snubber circuit inhibits excessive voltage increase, protecting the MOSFETs in the switching cell from overvoltage damage. The interval from short-circuit detection to full separation is 8.8  $\mu$ s, with the transient process lasting up to 25.6  $\mu$ s.

The overload protection mechanism resembles fault isolation during a short circuit (Fig. 10), with the sole difference being the timing. Short-circuit incidents necessitate prompt intervention, whereas overload protection is engaged with a delay to accommodate temporary overloads, in accordance with B characteristics. The overload protection test starts with normal SSCB operation under a 10 A load current, which is then increased to 20 A. Following a one-second delay, the overload is isolated.

The prototype SSCB power loss breakdown at a nominal load of 16 A and a light load of 1 A is shown in Fig. 11. The main sources of power loss are the transistors Q1 and Q2. The SSCB control system, consisting of a microcontroller, measurement circuits, and transistor drivers, consumes 0.37 W continuously. An additional 0.08 W is wasted in the primary 350 V DC to 12 V DC auxiliary power supply, resulting in an overall efficiency of 99.7% at nominal load and 99.8% at light load.

Through extensive testing, we established that the proposed DC RCD/SSCB hybrid offers reliable protection in residential DC microgrids, both against short circuits and by

safeguarding users from electric shock via detection of excessive residual current levels.

## 6. Conclusions

This article discusses the necessity for specialized protection devices that integrate short-circuit protection, residual current sensing, telemetry, and other features within emerging residential DC microgrids. It also outlines the associated implementation challenges and grid-side requirements. Based on this research, a hybrid bidirectional solid-state circuit breaker and residual current device was designed, fabricated, and tested. The proposed device is a hybrid of an SSCB and a RCD, which supports bidirectional current operation and allows integration into an energy management system. This functionality was achieved utilizing two back-to-back connected MOSFETs, a low-cost microcontroller, and a self-oscillation fluxgate residual current sensor. Current measurement was accomplished using an operational amplifier and a shunt resistor, while adaptable control and fault management were enabled by an economical and low-speed microprocessor paired with a trigger circuit. An external analog circuit comparator was employed for overcurrent detection. A fluxgate sensor featuring a closed loop and self-oscillating mechanism was employed to measure residual current. Integrated Wi-Fi and Bluetooth connectivity modules provide capabilities for remote load control and telemetry. The proposed design, capable of detecting residual currents above 6 mA, withstanding repeated short circuit events, and reacting to fault conditions in under 10  $\mu$ s, was experimentally validated. The prototype's features are sufficient to protect the power semiconductor converters supplying a DC microgrid and to safeguard users from electric shock, while maintaining high efficiency ( $>99\%$ ). Energy storage devices,

including batteries and supercapacitors, integrated into microgrids can be protected against overcurrent through bidirectional current switching capabilities.

Future research will concentrate on utilizing the advanced communication capabilities of the employed microcontroller to incorporate the proposed hybrid DC protection device into a smart and versatile energy management system.

#### Data availability statement

Data are contained within the article.

#### Acknowledgments

This work was supported in part by the Estonian Research Council under grant PRG1086 and in part by the Estonian Centre of Excellence in Energy Efficiency (ENER), funded by the Estonian Ministry of Education and Research under grant TK230. The publication costs of this article were partially covered by the Estonian Academy of Sciences.

#### References

- Attia, S., Kurnitski, J., Kosiński, P., Borodinecs, A., Deme Belafi, Z., István, K. et al. Overview and future challenges of nearly zero-energy building (nZEB) design in Eastern Europe. *Energy Build.*, 2022, **267**, 112165. <http://dx.doi.org/10.1016/j.enbuild.2022.112165>
- Carvalho, E. L., Blinov, A., Chub, A., Emiliani, P., de Carne, G. and Vinnikov, D. Grid integration of DC buildings: standards, requirements and power converter topologies. *IEEE Open J. Power Electron.*, 2022, **3**, 798–823. <https://doi.org/10.1109/OJPEL.2022.3217741>
- Chub, A., Vinnikov, D., Korkh, O., Malinowski, M. and Kouro, S. Ultrawide voltage gain range microconverter for integration of silicon and thin-film photovoltaic modules in DC microgrids. *IEEE Trans. Power Electron.*, 2021, **36**(12), 13763–13778. <https://doi.org/10.1109/TPEL.2021.3084918>
- Husev, O., Matiushkin, O., Vinnikov, D., Roncero-Clemente, C. and Kouro, S. Novel concept of solar converter with universal applicability for DC and AC microgrids. *IEEE Trans. Ind. Electron.*, 2022, **69**(5), 4329–4341. <https://doi.org/10.1109/TIE.2021.3086436>
- Nguyen, T. L. and Griepentrog, G. Modeling, control and stability analysis for a DC nanogrid system. In *2018 IEEE 19th Workshop on Control and Modeling for Power Electronics (COMPEL), Padua, Italy, 25–28 June 2018*. IEEE, 2018, 1–8.
- Abdel-Rahim, O., Chub, A., Vinnikov, D. and Blinov, A. DC integration of residential photovoltaic systems: a survey. *IEEE Access*, 2022, **10**, 66974–66991. <https://doi.org/10.1109/ACCESS.2022.3185788>
- Roasto, I., Blinov, A. and Vinnikov, D. Soft start algorithm for a droop controlled DC nanogrid. In *2022 18th Biennial Baltic Electronics Conference (BEC), Tallinn, Estonia, 4–6 October 2022*. IEEE, 2022, 1–6.
- Mackay, L., van der Blij, N. H., Ramirez-Elizondo, L and Bauer, P. Toward the universal DC distribution system. *Electr. Power Compon. Syst.*, 2017, **45**, 1032–1042. <https://doi.org/10.1080/15325008.2017.1318977>
- Wan, M., Dong, R., Yang, J., Xu, Z., Zhang, B. and He, K. Fault mechanism and protection strategy for DC micro-grid. In *2019 IEEE 28th International Symposium on Industrial Electronics (ISIE), Vancouver, Canada, 12–14 June 2019*. IEEE, 2019, 2597–2602.
- Patel, V. and Patel, V. A comprehensive review: AC & DC microgrid protection. In *2020 21st National Power Systems Conference (NPSC), Gandhinagar, India, 17–19 December 2020*. IEEE, 2020, 1–6.
- Dali, M., Charaabi, F. and Belhadj, J. Short-circuit fault analysis and protection of stand-alone AC and DC microgrids. In *2022 IEEE International Conference on Electrical Sciences and Technologies in Maghreb (CISTEM), Tunis, Tunisia, 26–28 October 2022*. IEEE, 2022, 1–6.
- Rodrigues, R., Du, Y., Antoniazzi, A. and Cairoli, P. A review of solid-state circuit breakers. *IEEE Trans. Power Electron.*, 2021, **36**(1), 364–377. <https://doi.org/10.1109/TPEL.2020.3003358>
- Shen, Z. J., Miao, Z. and Roshandeh, A. M. Solid state circuit breakers for DC microgrids: current status and future trends. In *2015 IEEE First International Conference on DC Microgrids (ICDCM), Atlanta, USA, 7–10 June 2015*. IEEE, 2015, 228–233.
- Anselmo, I. S. and Rashid, M. H. Solid-state circuit breakers for D.C. microgrid applications. In *2020 International Conference on Electrical, Communication, and Computer Engineering (ICECCE), Istanbul, Turkey, 12–13 June 2020*. IEEE, 2020, 1–4.
- Jalakas, T., Chub, A., Roasto, I. and Vinnikov, D. Hybrid residual current device and solid state circuit breaker for residential DC microgrids. In *2024 19th Biennial Baltic Electronics Conference (BEC), Tallinn, Estonia, 2–4 October 2024*. IEEE, 2024, 1–5.
- Royal Dutch Standardization Institute (NEN). *NL: DC Installations for Low Voltage Standard NPR 9090:2018*. 2018, 1–50.
- Rodriguez-Diaz, E., Chen, F., Vasquez, J. C., Guerrero, J. M., Burgos, R. and Boroyevich, D. Voltage-level selection of future two-level LV DC distribution grids: a compromise between grid compatibility, safety, and efficiency. *IEEE Electr. Mag.*, 2016, **4**(2), 20–28. <https://doi.org/10.1109/MELE.2016.2543979>
- Neyret, Y. *DC Microgrids: Principles and Benefits*. DC-Systems, 10–11, 2024. <https://www.dc.systems/assets/public/DC-Systems-White-Paper.pdf> (accessed 2024-11-24).
- Carvalho, E. L., Blinov, A., Chub, A., Emiliani, P., de Carne, G. and Vinnikov, D. Grid integration of DC buildings: standards, requirements and power converter topologies. *IEEE Open J. Power Electron.*, 2022, **3**, 798–823. <https://doi.org/10.1109/OJPEL.2022.3217741>
- International Electrotechnical Commission. *IEC 60364-5-52:2009 Low-voltage electrical installations – Part 5-52: Selection and erection of electrical equipment – Wiring systems*.
- Selamogullari, U. S. and Alsaad, A. Analysis of a residential distribution system with the application of conservation voltage reduction at house level. In *2019 1st Global Power, Energy and Communication Conference (GPECOM), Nevsehir, Turkey, 12–15 June 2019*. IEEE, 2019, 430–434.
- Palaniappan, K., Sedano, W., Vygoder, M., Hoefft, N., Cuzner, R. and Shen, Z. J. Short-circuit fault discrimination using SiC JFET-based self-powered solid-state circuit breakers in a residential DC community microgrid. *IEEE Trans. Ind. Appl.*, 2020, **56**(4), 3466–3476. <https://doi.org/10.1109/TIA.2020.2995114>
- Cuzner, R., MacFarlin, D., Clinger, D., Rumney, M. and Castles, G. Circuit breaker protection considerations in power converter-fed DC systems. In *IEEE Electric Ship Technologies Symposium, Baltimore, USA, 20–22 April 2009*. IEEE, 2009, 360–367.
- Rodrigues, R., Du, Y., Antoniazzi, A. and Cairoli, P. A review of solid-state circuit breakers. *IEEE Trans. Power Electron.*, 2020, **36**(1), 364–377. <https://doi.org/10.1109/TPEL.2020.3003358>
- International Electrotechnical Commission. *IEC 60898-1:2015/AMD1:2019/COR1:2020, Corrigendum 1 – Amendment 1 – Electrical accessories – Circuit-breakers for overcurrent protection for household and similar installations*.
- Shneider Electric. Acti9 C60H-DC datasheet. <https://www.se.com/in/en/product/A9N61531/minature-circuit-breaker-c60h-2-poles-16-a-c-curve> (accessed 2024-11-24).
- Zhang, L., Tai, N., Huang, W., Liu, J. and Wang, Y. A review on protection of DC microgrids. *J. Mod. Power Syst. Clean Energy*, 2018, **6**(6), 1113–1127. <https://doi.org/10.1007/s40565-018-0381-9>

28. Mohanty, R. and Pradhan, A. K. Protection of DC and hybrid AC-DC microgrids with ring configuration. In *2017 7th International Conference on Power Systems (ICPS), Pune, India, 21–23 December 2017*. IEEE, 2017, 607–612.
29. Salomonsson, D., Soder, L. and Sannino, A. Protection of low-voltage DC microgrids. *IEEE Trans. Power Deliv.*, 2009, **24**(3), 1045–1053. <https://doi.org/10.1109/TPWRD.2009.2016622>
30. Miao, Z., Sabui, G., Moradkhani Roshandeh, A. and Shen, Z. J. Design and analysis of DC solid-state circuit breakers using SiC JFETs. *IEEE J. Emerg. Sel. Top. Power Electron.*, 2016, **4**(3), 863–873. <https://doi.org/10.1109/JESTPE.2016.2558448>
31. Xu, X., Chen, W., Tao, H., Zhou, Q., Li, Z. and Zhang, B. Design and experimental verification of an efficient SSCB based on CS-MCT. *IEEE Trans. Power Electron.*, 2020, **35**(11), 11682–11693. <https://doi.org/10.1109/TPEL.2020.2987418>
32. Swamy, S. N. and Kota, S. R. An empirical study on system level aspects of Internet of Things (IoT). *IEEE Access*, 2020, **8**, 188082–188134. <https://doi.org/10.1109/ACCESS.2020.3029847>
33. Ding, J., Nemati, M., Ranaweera, C. and Choi, J. IoT connectivity technologies and applications: a survey. *IEEE Access*, 2020, **8**, 67646–67673. <https://doi.org/10.1109/ACCESS.2020.2985932>
34. Buffolo, M., Favero, D., Marcuzzi, A., De Santi, C., Menghesso, G. and Zanoni, E. Review and outlook on GaN and SiC power devices: industrial state-of-the-art, applications, and perspectives. *IEEE Trans. Electron Devices*, 2024, **71**(3), 1344–1355. <https://doi.org/10.1109/TED.2023.3346369>
35. She, X., Huang, A. Q., Lucia, Ó. and Ozpineci, B. Review of silicon carbide power devices and their applications. *IEEE Trans. Ind. Electron.*, 2017, **64**(10), 8193–8205. <https://doi.org/10.1109/TIE.2017.2652401>
36. Jalakas, T., Chub, A., Roasto, I. and Vinnikov, D. Design of solid state circuit breaker. In *2022 IEEE 63th International Scientific Conference on Power and Electrical Engineering of Riga Technical University (RTUCON), Riga, Latvia, 10–12 October 2022*. IEEE, 2022, 1–5.
37. Guiyong, Z., Huaicheng, W., Yu, D., Yanhe, S., Xiaomou, L. and Chuang, B. Design and implementation of high-precision current measurement instrument based on hall sensor. In *2023 20th International Computer Conference on Wavelet Active Media Technology and Information Processing (ICCWAMTIP), Chengdu, China, 15–17 December 2023*. IEEE, 2023, 1–5.
38. Yang, W., Zhuo, Y. and Anheuser, M. A residual current measurement method with a combination of MR and Hall effect sensors. In *2010 IEEE International Workshop on Applied Measurements for Power Systems, Aachen, Germany, 22–24 September 2010*. IEEE, 2010, 27–30.
39. Namia-Cohen, Y., Sharon, Y., Khachatryan, B. and Cheskis, D. DC low current Hall effect measurements. In *2018 IEEE International Conference on the Science of Electrical Engineering in Israel (ICSEE), Eilat, Israel, 12–14 December 2018*. IEEE, 2018, 1–4.
40. Oliveira, T. R. Design of a low-cost residual current sensor for LVDC power distribution application. In *2018 13th IEEE International Conference on Industry Applications (INDUSCON), Sao Paulo, Brazil, 12–14 November 2018*. IEEE, 2018, 1313–1319.
41. Ding, Z., Wang, J., Li, C., Wang, K. and Shao, H. A wideband closed-loop residual current sensor based on self-oscillating fluxgate. *IEEE Access*, 2023, **11**, 134126–134135. <https://doi.org/10.1109/ACCESS.2023.3335653>
42. Kondalkar, V. V., Li, X., Yang, S. S. and Lee, K. Towards a wireless chip less smart current sensor system based on giant magnetoresistance. In *2017 19th International Conference on Solid-State Sensors, Actuators and Microsystems (TRANSDUCERS), Kaohsiung, Taiwan, 18–22 June 2017*. IEEE, 2017, 1092–1095.
43. Xie, F., Weiss, R. and Weigel, R. Giant-magnetoresistance-based galvanically isolated voltage and current measurements. *IEEE Trans. Instrum. Meas.*, 2015, **64**(8), 2048–2054. <https://doi.org/10.1109/TIM.2015.2440553>
44. Cheng, D., Zhang, B., Xiong, S., Xie, Z. and Xue, Z. Residual current detection prototype and simulation method in low voltage DC system. *IEEE Access*, 2022, **10**, 51100–51109. <https://doi.org/10.1109/ACCESS.2022.3172698>
45. IEC 61660-1:1997. *Short-circuit currents in d.c. auxiliary installations in power plants and substations – Part 1: Calculation of short-circuit currents*.
46. Emhemed, A. and Burt, G. The effectiveness of using IEC61660 for characterising short-circuit currents of future low voltage DC distribution networks. In *22nd International Conference and Exhibition on Electricity Distribution (CIRED 2013), Stockholm, Sweden, 10–13 June 2013*. IEEE, 2013, 1330.

## Majapidamiste alalisvoolu mikrovõrkude pooljuhtkaitselülite disain ja arendus

Tanel Jalakas, Andrii Chub, Indrek Roasto, Dmitri Vinnikov ja Jarek Kurnitski

Majapidamiste alalisvoolu mikrovõrgud vajavad kiireid ja usaldusväärseid tehnoloogilisi lahendusi rikkevoolu tuvastamiseks ning kaitseks ülekoormuse, liigvoolu ja ülepinge eest. Alalisvoolu mikrovõrgud, mida sageli isoleerustab suur mahtuvus ja madal induktiivsus, ei ühildu hästi traditsiooniliste sulavkaitsmete, elektrotermiliste kaitselülite ja rikkevoolu tuvastamise seadmetega, mis on mõeldud kasutamiseks vahelduvvoolu energiasüsteemides. Lahendust sellele probleemile pakuvad pooljuhtkaitselülid. Mikrokontrolleripõhised juhtahelad koos mitmesuguste anduritega hõlbustavad rikete kiiret tuvastamist, võrgu parameetrite mõõtmist, telemetriat ja koormuste juhtimist, samas kui väljatransistoride põhised lülituselemendid võimaldavad rikked kiiresti võrgust eraldada. Selliste nõuete täitmiseks on vaja seadet, mis integreerib pooljuhtkaitselüliti ja rikkevoolukaitsese funktsioonid ühte hübriidseadmesse. Voolu ja pinget kiire mõõtmine on väga lihtne, ent kasutajate ja ühendatud seadmete kaitsmiseks on vaja ka töökindlaid meetodeid alalisvoolu jääkvoolu mõõtmiseks. Alalisvooluvõrkudes saab rikkevoolu mõõtmiseks otse kasutada vaid piiratud arvu lahendusi. Väikeste lekkevoolude mõõtmiseks on vaja kas fluxgate-tüüpi või Halli efekti andurit või mõnda muud alternatiivset aktiivset anduritehnoloogiat. Halli efekti andurid on energiatõhusad ja kompaktsed, samas kui fluxgate-tüüpi vooluandurid tagavad parema lineaarsuse ja täpsuse. Seetõttu soovitatakse välja töötada hübriid-alalisvoolukaitseseade, mis toimiks nii pooljuhtkaitselüliti kui ka rikkevooluandurina. Pakutud hübriidseadme hindamiseks uuriti alalisvoolu mikrovõrkude ja erinevate rikkevoolu mõõtmistehnikate projekteerimise ja rakendamise aspekte, valiti sobiv toiteahela topoloogia, töötati välja kompaktne prototüüp ja hinnati selle toimivust laboratoorses tingimustes. Läbiviidud testid näitasid seadme vastavust nõuetele, kasulikkust elamute 350 V alalisvoolu mikrovõrkudes ning võimet kaitsta mikro- võrku lühiste ja selle kasutajaid elektrilöögi eest ning võrku ühendatud seadmeid ülekoormuse eest.